

RESEARCH ARTICLE

RAB31 drives extracellular vesicle fusion and cancer-associated fibroblast formation leading to oxaliplatin resistance in colorectal cancer

Yu-Chan Chang¹ | Yi-Fang Yang² | Chien-Hsiu Li³ | Ming-Hsien Chan¹ |
Meng-Lun Lu⁴ | Ming-Huang Chen^{4,5,6} | Chi-Long Chen^{7,8} | Michael Hsiao³ 

¹Department of Biomedical Imaging and Radiological Sciences, National Yang Ming Chiao Tung University, Taipei, Taiwan

²Department of Medical Education and Research, Kaohsiung Veterans General Hospital, Kaohsiung, Taiwan

³Genomics Research Center, Academia Sinica, Taipei, Taiwan

⁴Department of Oncology, Taipei Veterans General Hospital, Taipei, Taiwan

⁵School of Medicine, National Yang Ming Chiao Tung University, Taipei, Taiwan

⁶Center of Immuno-Oncology, Department of Oncology, Taipei Veterans General Hospital, Taipei, Taiwan

⁷Department of Pathology, Taipei Medical University Hospital, Taipei Medical University, Taipei, Taiwan

⁸Department of Pathology, College of Medicine, Taipei Medical University, Taipei, Taiwan

Correspondence

Dr. Chi-Long Chen, Department of Pathology, Taipei Medical University Hospital, Taipei Medical University, Taipei, Taiwan.
Email: chencl@tmu.edu.tw

Dr. Michael Hsiao, Genomics Research Center, Academia Sinica, 128 Academia Rd., Sec. 2, Nankang-Dist., Taipei, Taiwan.
Email: mhsiao@gate.sinica.edu.tw

Abstract

Epithelial-mesenchymal transition (EMT) is associated with tumorigenesis and drug resistance. The Rab superfamily of small G-proteins plays a role in regulating cell cytoskeleton and vesicle transport. However, it is not yet clear how the Rab family contributes to cancer progression by participating in EMT. By analysing various in silico datasets, we identified a statistically significant increase in *RAB31* expression in the oxaliplatin-resistant group compared to that in the parental or other chemotherapy drug groups. Our findings highlight *RAB31*'s powerful effect on colorectal cancer cell lines when compared with other family members. In a study that analysed multiple online meta-databases, *RAB31* RNA levels were continually detected in colorectal tissue arrays. Additionally, *RAB31* protein levels were correlated with various clinical parameters in clinical databases and were associated with negative prognoses for patients. *RAB31* expression levels in all three probes were calculated using a computer algorithm and were found to be positively correlated with EMT scores. The expression of the epithelial-type marker CDH1 was suppressed in *RAB31* overexpression models, whereas the expression of the mesenchymal-type markers SNAI1 and SNAI2 increased. Notably, *RAB31*-induced EMT and drug resistance are dependent on extracellular vesicle (EV) secretion. Interactome analysis confirmed that *RAB31*/AGR2 axis-mediated exocytosis was responsible for maintaining colorectal cell resistance to oxaliplatin. Our study concluded that *RAB31* alters the sensitivity of oxaliplatin, a supplementary chemotherapy approach, and is an independent prognostic factor that can be used in the treatment of colorectal cancer.

KEYWORDS

AGR2, colon cancer, epithelial-mesenchymal transition, oxaliplatin resistance, RAB31

1 | INTRODUCTION

Colorectal cancer is highly diagnosed and prevalent, with a significant number of cases (Siegel et al., 2022). On average, approximately 30% of patients with colon cancer are diagnosed with synchronous or metachronous metastases (Engstrand et al., 2018). For patients with metastatic colon cancer, commonly prescribed adjuvant chemotherapy drugs include irinotecan and oxaliplatin (Abrams et al., 2014). However, the development of chemoresistance leads to tumour recurrence and decreased survival rates. Therefore, understanding the causes of resistance and the complete mechanism will help patients to consider alternative

This is an open access article under the terms of the [Creative Commons Attribution-NonCommercial License](https://creativecommons.org/licenses/by-nc/4.0/), which permits use, distribution and reproduction in any medium, provided the original work is properly cited and is not used for commercial purposes.

© 2024 The Authors. *Journal of Extracellular Biology* published by Wiley Periodicals LLC on behalf of International Society for Extracellular Vesicles.

treatment options. Drug resistance is often the leading cause of treatment failure in patients with relapsing cancer. In this case, the ineffectiveness of the drug can result from both its activity and the cell's ability to transport it outside the cell (Wilson et al., 2006). Research has indicated that long-term exposure of colorectal cancer cells to oxaliplatin induces epithelial-to-mesenchymal transition (EMT) processes, such as the reduction of E-cadherin and the increase in Snail or vimentin, which enables the cells to resist efficacy (Yang et al., 2006). In colorectal cancer, EMT is the primary mechanism that promotes early invasion and metastasis (Tadosi et al., 2012). Multiple clinical studies have consistently demonstrated that a lack of E-cadherin is associated with a poorer prognosis and malignancy in colorectal cancers (Ye et al., 2015). Recently, it was demonstrated that tumour cells alter the basis of EMT and reprogram the tumour microenvironment (Spano & Zollo, 2012). One of the significant mechanisms resulting in oxaliplatin resistance in colorectal cancer is extracellular vesicle (EV) secretion (Han et al., 2020; Liu et al., 2019). Therefore, it is critical to identify the specific molecules that can trigger EMT and influence oxaliplatin resistance, thereby inhibiting early metastasis.

The Rab family of small GTPases is a member of the Ras superfamily. In the human body, Rab GTPase regulates vesicle trafficking and recycling by converting between the guanosine diphosphate (GDP) and guanosine triphosphate (GTP) forms (Homma et al., 2021). Each member of the Rab family performs unique functions, and has distinct distributions and expressions. Some members exhibit coordinated functionality, whereas others are redundant (Hutter, 2007; Martínez-Morales et al., 2022). Studies indicate that aberrant Rab expression during tumorigenesis is a significant, independent prognostic/diagnostic factor (Jin et al., 2021). Scientists have suggested that Rabs regulate oncogenic pathways or act as co-activators with several transcription factors (Erami et al., 2017; Stenmark, 2009). Recent discoveries regarding Rabs and their protein-interacting partners have confirmed their importance in cancer and other diseases (Chang et al., 2023). In colorectal cancer, Rab3C expression is associated with tumour metastasis via the STAT3/IL-6 axis (Chang et al., 2017). *RAB31* has also been reported to contribute to endosomal trafficking and the endosomal sorting complex required for the transport (ESCRT)-independent EV pathway (Jalagadugula et al., 2022; Wei et al., 2021), a more detailed mechanism has not been investigated.

This study focused on the expression of the *RAB31* gene in colorectal cells, utilising a series of clinical correlation selection procedures. Although *RAB31* plays a crucial role in vesicle- and granule-targeting, its involvement in the EMT pathway and drug resistance has been observed. It is noteworthy that this observation has only been made for *RAB31*, and none of the other Rabs have demonstrated this association. We identified new pathways and phenotypes that differed from previously reported canonical pathways. Additionally, we uncovered a unique function of *RAB31* in colorectal cancer.

2 | MATERIAL AND METHODS

2.1 | Cell lines and stable clones

Eight human colon cancer cell lines, three of which (CX-1, DLD-1 and H3347) were maintained in RPMI-1640 medium and two cell lines (HCT116 and HT-29) were maintained in McCoy's 5A modified medium (Sigma, St. Louis, MO, USA). The medium was supplemented with 10% fetal bovine serum (GIBCO, Grand Island, NY, USA), penicillin (100 units/mL) and streptomycin (100 µg/mL). Cells were incubated in a humidified atmosphere of 95% air, 5% CO₂ at 37°C. SW48, SW480 and SW620 cells were cultured in Leibovitz L-15 medium (Sigma, St. Louis, MO, USA) and incubated in a CO₂-free incubator. The L-15 medium formula is designed for free gas exchange with the atmosphere. When using this medium for culture, the mixture of CO₂ and air is harmful to cells, so these cells were cultured in a CO₂-free incubator. Human Colonic Fibroblasts were purchased from ScienceCell company (Cat#2880) and maintained in Fibroblast Medium (FM, Cat #2301, ScienCell, Carlsbad, CA, USA)

2.2 | Gene construction and lentivirus production

The lentiviral envelope and packing plasmids (pMDG and p Δ 8.91) were purchased from the National RNAi Core Facility (Academia Sinica, Taiwan). The pDONR223_*RAB31* lentiviral construct and empty vector were purchased from Addgene (Watertown, MA, USA) and swapped in a lentiviral backbone-based system. Lentiviruses were co-transfected into 293 T cells with pMDG ($p = 8.91$) and the plasmid construct using the calcium phosphate transfection method. After 48 h of incubation, the lentiviruses were collected and used to infect cells with polybrene (2 µg/mL). For two weeks, cells with altered *RAB31* expression were selected using blasticidin (2 µg/mL). Finally, a plasmid carrying a vector control sequence was used to create control cells.

2.3 | Cell viability measurements

Cell viability was determined using the TACS tetrazolium salt 3-(4,5-dimethylthiazol-2-yl)-2, 5-diphenyltetrazolium bromide (MTT) cell proliferation assay kit (Trevigen, Gaithersburg, MD, USA), according to the manufacturer's instructions. The MTT

assay was used to determine cell viability in cell proliferation and cytotoxicity assays. The cells were seeded at a concentration of 2000 cells/100 μ L of culture medium per well in 96-well microplates. At 24 h post-seeding, the cells were treated with the dimethyl sulfoxide (DMSO) solvent control or different doses of oxaliplatin/GW4869 for 24, 48 or 72 h. Subsequently, the cells were incubated in a medium containing MTT for 4 h, lysed with DMSO, and optical density at 570 nm was measured using a microplate reader (Spectral Max250; Molecular Devices, Sunnyvale, CA, USA).

2.4 | Electron microscopy and multivesicular body (MVB) quantification

The cells were washed in phosphate buffered saline (PBS) and fixed for 1 h in 2.5% glutaraldehyde in 0.1 M phosphate buffer at room temperature. Then, the cells were slowly and gently scraped and pelleted in Eppendorf tubes. We washed the pellets in phosphate buffer and incubated them with 1% OsO₄ for 90 min at 4°C. The samples were then dehydrated, embedded in Spurr, and sectioned using a Leica ultramicrotome (Leica Microsystems) (Edgar, 2016; Villarroja-Beltri et al., 2016). Ultrathin sections (50–70 nm) were stained with 2% uranyl acetate for 10 min, followed by a lead staining solution for 5 min, and observed using a transmission electron microscope (Hitachi TEM system). ImageJ software was used for calibration, quantification and analysis of the images. We identified MVBs and counted them by morphology, with only discrete ILVs. Lysosomes showed a multilayer morphology. We analysed at least 20 MVBs per experiment, using separate cells. We analysed the data from duplicate or triplicate experiments and used two to four grids for each condition. The minimum number of cells scored under each condition was 20. We generated box scatter plots using Prism GraphPad software and performed statistical tests in Microsoft Excel (calibration: 2.0; magnification: $\times 2.0$ K– $\times 6.0$ K; lens mode: Zoom-I; acc. voltage: 75.0 kV; emission: 5.8 μ A. Data are presented as mean \pm standard deviation; *** *p*-value < 0.0001.

2.5 | Nanoparticle tracking analysis

We used a nanoparticle tracking analysis (NTA) system to analyse the particle size distribution of the EV sample. The system was equipped with a 488 nm laser and a high-sensitivity scientific CMOS camera, and was used with a NanoSight NS300 system (Malvern Technologies, Malvern, UK). According to the manufacturer's specifications, we diluted the sample at 1:100 in particle-free PBS to an acceptable recommended concentration to reduce the number of particles in the field of view to below 100/frame. We recorded the reading videos in a single capture for 60 s at 30 frames per second (fps), with the camera level set to 15 and manual temperature monitoring. Then, we used NTA 3.1.54 software to divide the particle size distribution into 10 nm wide intervals, which was used for all the video reproductions to determine the concentration measurement value. To understand the variability in the estimated value within the entire interval width, the software organized the statistical data obtained from each frame.

2.6 | Western blot analysis

The cells were lysed in RIPA buffer for 30 min and then centrifuged at 13,000 rpm for 15 min at 4°C. Protein concentrations were measured using Bicinchoninic acid assay (BCA assay) protein assay reagent (Thermo Fisher Scientific, Waltham, MA, USA). Total proteins (30 μ g) were separated by SDS Poly-acrylamide-gel-electrophoresis (SDS-PAGE) on 10% polyacrylamide gels and transferred to (lyvinylidene fluoride a PVDF) membranes. The membranes were hybridised with primary antibodies overnight after blocking for 30 min in 5% non-fat milk. The samples were incubated with secondary antibodies for 1 h, and the proteins were visualised using enhanced chemiluminescence reagents (ECL) (Perkin Elmer, Waltham, MA, USA). Quantitative data were obtained using ImageJ software.

Western blot analysis was performed using the following primary antibodies: anti-*RAB31* (1:1000) (Cat # 15485-1-AP, Proteintech, Rosemont, IL, USA), anti-pEGFR tyr 1173 (1:1000) (Cat # ab32578, Abcam), anti-EGFR (1:1000) (Cat # ab32198, Abcam), anti-pErk thr 202 (1:1000) (Cat # ab201015, Abcam), anti-Erk (1:1000) (Cat # ab32537, Abcam), anti-pAkt ser 473 (1:1000) (cat. no: 4060, Cell Signaling Technology), anti-Akt (1:2000) (cat. no: 4691, Cell Signaling Technology), anti-Slug (1:1000) (cat. no: 9585, Cell Signaling Technology), anti-E-cadherin (1:1000) (cat. no.610182, BD Biosciences), anti-TSG101 (1:1000) (Cat # ab125011, Abcam), anti-VPS24 (1:1000) (Cat # 15472-1-AP, Proteintech), anti-VPS28 (1:1000) (Cat # 15478-1-AP, Proteintech), anti-CD9 (1:5000) (Cat # sc-6327, Sdanta Cruz), anti-CHMP4B (1:1000) (Cat # 42466, Cell Signaling Technology), anti-FLOT1 (1:2000) (Cat # ab41927, Abcam), anti-FLOT2 (1:2000) (Cat # 3244, Cell Signaling Technology), anti-CD63 (1:1000) (Cat # ab231975, Abcam), anti-TBC1D2B (1:1000) (Cat # ab185102, Abcam) anti-calnexin (1:1000) (Cat # ab92573, Abcam), anti-vimentin (1:1000) (Cat # ab92547, Abcam), and anti- α -tubulin (1:104) (Sigma-Aldrich, St. Louis, MO, USA).

2.7 | EV isolation and extraction

According to traditional ultra-high-speed centrifugation, the exosomal fraction from the filtered fluid of the cell culture medium was isolated. Briefly, cancer cells and debris were removed from the conditioned medium by centrifugation at 500×g for 10 min and 2000×g for 30 min. The supernatant was then filtered through a 0.22- μ m filter and ultra-high-speed centrifuged at 100,000×g for 90 min (Beckman 70Ti rotor). Finally, the isolated EV pellets were resuspended and washed three times with PBS through Amicon-0.5 mL centrifugal filters (100 kDa, Millipore, Billerica, MA, USA) for concentration and further analysis. These procedures have also been described in previous studies (Chang et al., 2020).

2.8 | Exosome membrane labelling

Researchers commonly use fluorescent dyes to label the cellular membrane during exosome labelling because the lipid bilayers in exosomes are a good target. Here, we chose the ExoParkler Exosome Membrane Labeling Lit-Red (Dojindo, Kumamoto, Japan), which enabled us to use the application to experiment using multiple labels. After collecting 10^9 – 10^{10} exosomes suspended in 100 μ L PBS, we added 2 μ L Mem Dye stock solution and mixed it with the exosomes. We transferred the staining exosomes to a filtration tube and centrifuged them at 3000×g for 5 mins about three times. We added 50 μ L of PBS to recover the labelled exosomes.

2.9 | Immunoprecipitation and immunoblotting analyses

Whole-cell lysates (2 mg) from cultured cells were incubated overnight in IP buffer with 25 μ L of protein A/G magnetic beads and the corresponding antibodies against *RAB31* (Cat # 15485-1-AP, Proteintech, Rosemont, IL, USA) or *AGR2* (Cat # GTX00601, GeneTex, Hsinchu, Taiwan) in a 1.5 mL microcentrifuge tube with a final volume of 1000 μ L. Proteins interacting with the antibodies were purified according to the manufacturer's protocol.

2.10 | Migration/Invasion assay

For migration/invasion assays, we coated 8 μ m-pore-size polycarbonate filters (GE Healthcare Life Sciences, Chalfont St. Giles, UK) with 1 mg/mL human fibronectin (Sigma, St. Louis, MO, USA). Alternatively, if the other side is coated with Matrigel, it is used for invasion experiments. We added medium containing 10% FBS to the lower compartment, and cells suspended in serum-free medium were added to the upper compartment of the Boyden chamber. After optimal timing (12–16 h), the migrating cells were stained with Giemsa solution and counted under a light microscope (400×, eight random fields of each well) for further quantification. We performed three independent experiments, each with four replicates. Count the number of Giemsa-stained cells in each field of view and take the percentage, with the control group as the baseline. The detailed process and classification are introduced in our previous study (Chang et al., 2019).

2.11 | Luciferase reporter assay

CRC cancer cells were transfected with 0.5 μ g of reporter containing E-cadherin sequence inserted upstream of the firefly luciferase gene in the pGL3 enhancer plasmid vector. As an internal standard, all plasmids were co-transfected with pRL-TK, which contains the Renilla luciferase gene. Cells were collected 48 h after transfection, and cell lysates were prepared according to Promega's instruction manual. The luciferase signals were measured by using a plate reader and One-Glo luciferase reagent (#E6120, Promega, Madison, WI, USA).

2.12 | Synergy calculation

We formulated all dosing groups in a dose-dependent manner from 1 nM to 100 μ M to calculate the cell viability percentages. These values were uploaded to the SynergyFinder website for statistical analysis (<https://synergyfinder.fimm.fi/>). We present the synergy scores and degrees of inhibition for the two compounds based on available algorithms (synergy score (δ -score) < 10: antagonistic; –10–10: additive; > 10: synergistic).

2.13 | Statistical analysis

The non-parametric Mann-Whitney U -test was used to analyse the statistical significance of the results from three independent experiments. Statistical analyses were performed using SPSS (Statistical Package for the Social Sciences) 17.0 software (version 17.0; SPSS, Chicago, IL, USA). For all analyses, a p -value of < 0.05 was considered significant.

3 | RESULTS

3.1 | *RAB31* expression confers resistance to oxaliplatin and serves as an independent prognostic marker

To discern chemoresistance events among therapeutic treatments for colorectal cancer and identify potentially involved genes, we analysed the GEO dataset (GSE42387), which includes commonly used drugs such as oxaliplatin and irinotecan for advanced and metastatic colorectal cancers. After normalisation and selection of an appropriate cutoff (1.5-fold change), we used a Venn diagram to identify genes affected by oxaliplatin and irinotecan in the two colorectal cancer files (Figure 1a). The findings revealed significant alterations in several probes in the oxaliplatin-resistant group when compared to the irinotecan-resistant and parental groups. Among HT-29 and LoVo cells, 342 (in red) and 531 (in blue) genes were identified. After merging and selecting common features, we isolated 18 candidates for further experimentation. Among these probes, *RAB31* ranked high and multiple groups of probes showed similar trends (Figure 1b). Previous research has shown that *RAB31* is involved in oxaliplatin resistance and is associated with a high risk of colorectal cancer (Zheng et al., 2015). Forest plots are revealing that *RAB31* expression is associated with a high risk ratio in colorectal cancer cohorts, similar to other significant prognostic variables. We found *RAB31* to be the only statistically significant candidate among the Rab family in this dataset. To verify that *RAB31* expression is not specific to HT-29 and LoVo cells, we analysed multiple GEO datasets (GSE30011 and GSE10405). These findings indicate that several colorectal cancer cell lines induced *RAB31* expression following exposure to oxaliplatin (Figure 1d). Compared to the other candidates, *RAB31* exhibited a more prominent trend in multiple cell models (Figure S1). Additionally, a meta-cohort analysis of clinical data showed a significant elevation of *RAB31* expression in colorectal carcinomas ($p = 9.78e-05$) (Figure 1e). Therefore, upregulation of *RAB31* expression in colorectal cancer could be linked to oxaliplatin resistance. From a clinical perspective, it is worth noting that *RAB31* has prognostic value in relation to both the overall survival rate and disease-free survival rate (Figure S2A,B). Interestingly, independent cohorts using chemotherapy demonstrated a significant effect on the outcomes of patients receiving chemotherapy (Figure S2C).

3.2 | *RAB31* exhibits heterogeneity and exocytotic properties in colorectal cancer

To examine the expression and characteristics of *RAB31* in colorectal models, we obtained endogenous expression levels of *RAB31* mRNA from the COAD panel on TCGA website (Figure 2a). Additionally, we measured the expression of *RAB31* in our cellular model (Figure 2b), providing evidence of consistent trends and differential baselines for *RAB31* across each cell line (Figure 2b). Based on these expression profiles, we selected CX-1 and HT-29 as overexpressing cells. Both quantitative polymerase chain reaction (qPCR) and western blot assays verified the overexpression of varying concentrations of *RAB31* cDNA in CX-1 and HT-29 cells (Figure 2c,d).

Rab proteins play crucial roles in various biological functions such as vesicle trafficking and exocytosis (Hendrix & Hume, 2011; Jin et al., 2021). *RAB31* is an exocytotic RAB protein known for its effect on the extent and efficiency of exocytosis when overexpressed. Some literature has suggested that *RAB31* is incorporated into exosomes and leaves cells (Wei et al., 2021). We tried to isolate extracellular vesicle (EV) and compare them with total lysate. EVs were isolated and analysed for the presence of positive markers (TSG101) or negative markers (calnexin). Upon overexpression of *RAB31*, EVs showed the presence of *RAB31* protein at higher levels than total lysate, as shown by qPCR and immunoblotting (Figure 2e,f). Instead, the exocytosis inhibitor GW4869 was used to interfere with this process. Our findings indicated that GW4869 partially inhibited the expression of *RAB31* (Figure 2g). In addition, some mRNA, microRNA and natural antisense RNA including *HMB5*, *B2M*, *RPL13A*, miR-21 and miR-192 in CRC cell line exosomes have been detected and compared in previously published literature (Chiba et al., 2012). We incorporated these molecules and observed that these entities were downregulated following GW4869 intervention (Figure S3). Therefore, *RAB31* expression controls the degree of exocytosis in CRC cell lines of colorectal cancer.

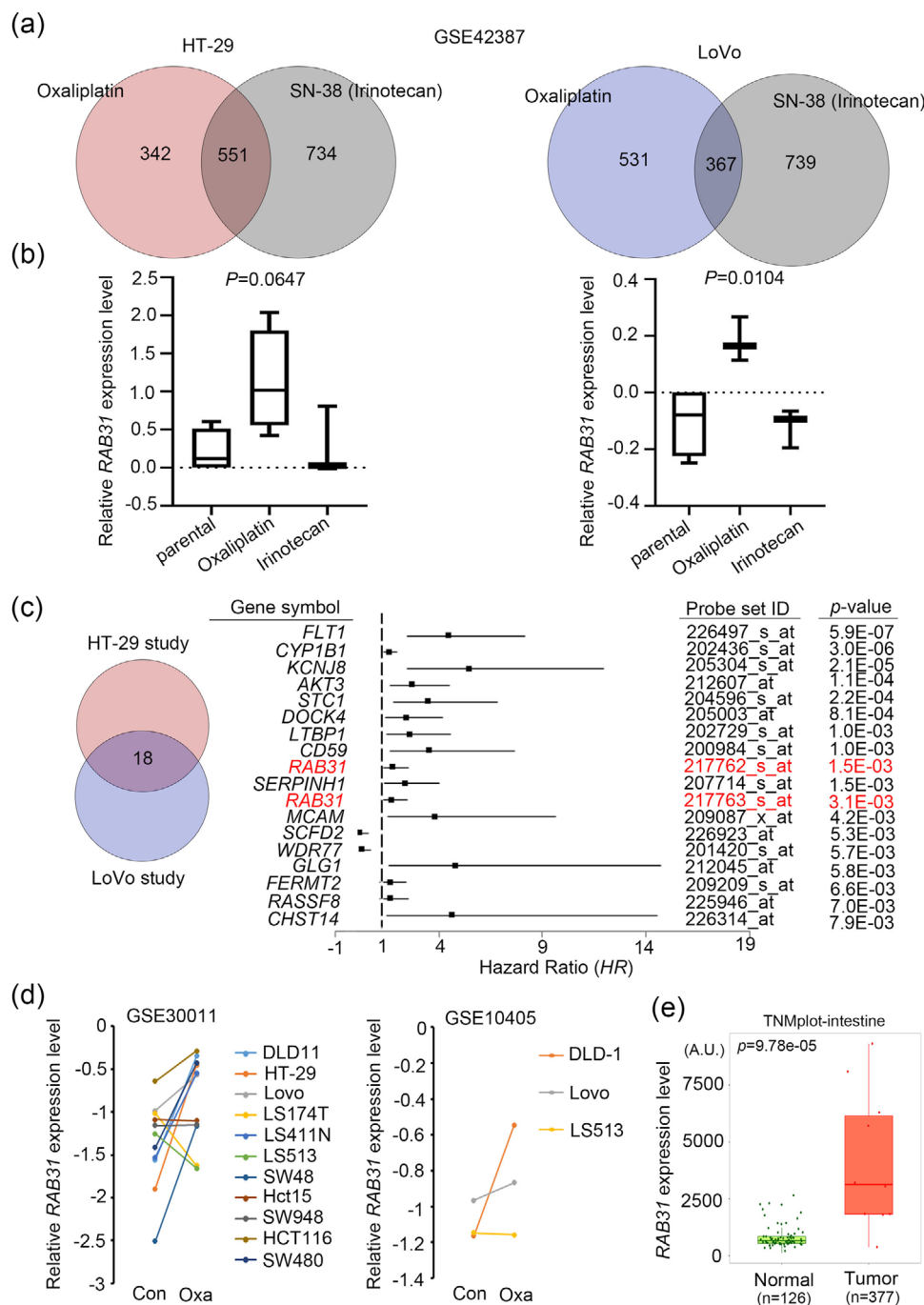


FIGURE 1 *RAB31* as a predictor of oxaliplatin resistance in colorectal cancer. (a) Venn diagram showing significant changes in targets between oxaliplatin resistance or SN-38 (Irinotecan)-resistance HT-29 and LoVo cells compared to the parental group, respectively. All raw data analyses are from GSE42387. (b) Boxplot showing the expression levels between the three events in (a). (c) The forest plot that predicts prognosis markers in the colorectal cancer cohort and their corresponding risk ratios, p -values, and probe IDs. (d) The levels of expression for *RAB31* were analysed in both treated and oxaliplatin-resistant colorectal cancer cell lines in various datasets (GSE30011 and GSE10405). (e) *RAB31* expression levels were evaluated in a colorectal cancer meta-cohort, obtained from the TNMplot website (Bartha & Györfy, 2021). The significance of the difference was determined using a non-parametric Mann-Whitney U test.

3.3 | *RAB31*-induced exocytosis confers oxaliplatin resistance to colorectal cancer cells

To confirm the potential connection between *RAB31* expression and oxaliplatin resistance, we modelled oxaliplatin IC50 values in colorectal cancer cell lines using the Genomics of Drug Sensitivity in Cancer (GDSC) website (Figure 3a). We selected several colorectal cancer cell lines, including SW1116, LS-123, and HT-29, for further experimentation. Of these, SW1116 and LS-123 were

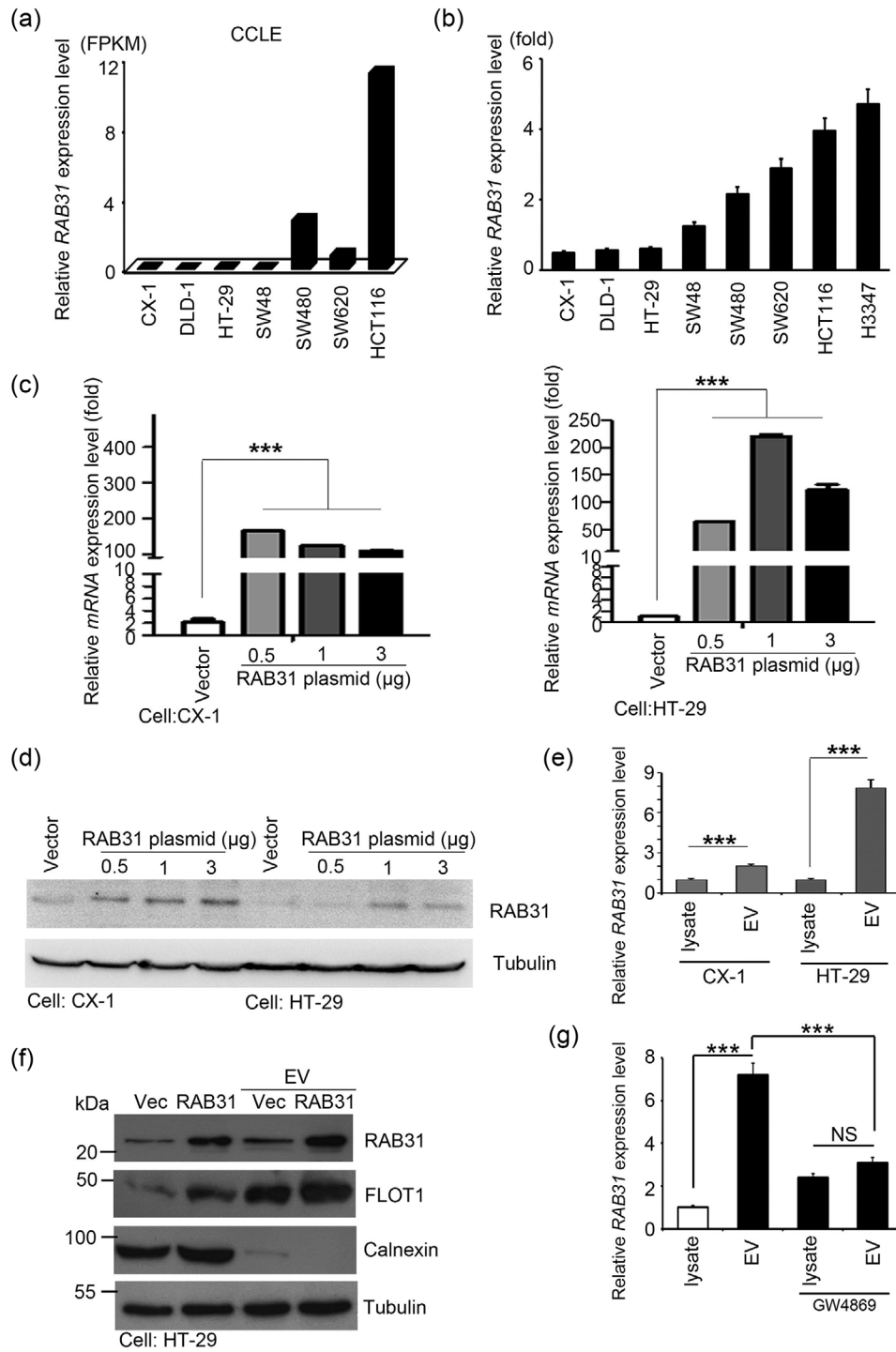


FIGURE 2 High expression and secretion of *RAB31* is observed in malignant cells. (a) Boxplot showing the expression levels of *RAB31* mRNA in colorectal cancer cells detected by next-generation sequencing from the Cancer Cell Line Encyclopedia (CCLE) dataset. (b) qPCR analysis was performed on *RAB31* expression in the collected colorectal cancer cell panel collected. (c) qPCR results showing the overexpression vector or gradient expression of *RAB31* in CX-1 and HT-29 cells, respectively. (d) Western blots detected *RAB31* expression with vector or gradient *RAB31* expression in CX-1 and HT-29 cells, respectively. (e) qPCR results of *RAB31* expression in total lysates or EV isolates performed in CX-1 and HT-29 *RAB31* overexpressing cells, respectively. (f) Western blots that detect *RAB31* expression and EV-related molecules in total lysates or isolation of EV from HT-29 cells. (g) qPCR detection of *RAB31* expression levels in total lysates or EVs from HT-29 overexpressing cells treated with or without GW4869. EV, extracellular vesicle; qPCR, quantitative polymerase chain reaction. *** $p < 0.001$ compared to vehicle group by Student's *t*-test.

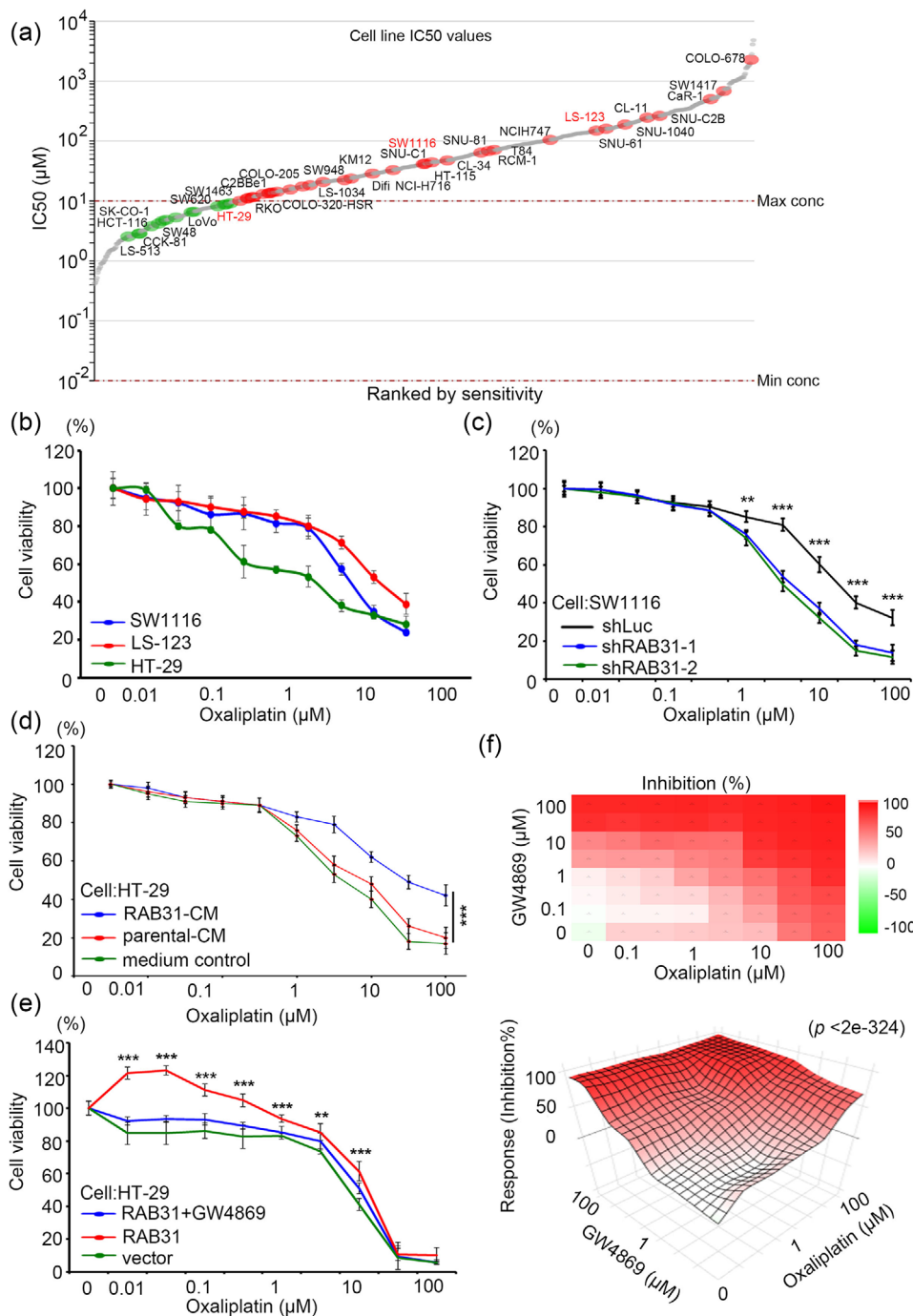


FIGURE 3 *RAB31* secretion and expression are the main factors involved in the resistance of colon cancer cells to oxaliplatin. (a) The IC₅₀ values for oxaliplatin were determined in various colon cancer cell lines. Drug resistance was indicated as red, while drug sensitivity was indicated as green. (b) The alamarBlue assay is used to measure the cell viability of various colon cancer cell lines treated with oxaliplatin (0.01–100 μM), including HT-29, HCT-116, and SW620 cells. (c) The alamarBlue assay was used to measure the cell viability of SW1116 cells with or without *RAB31* knockdown clones and treated with oxaliplatin. Two independent knockdown clones, shRAB31-1 and shRAB31-2. (d) The alamarBlue assay was used to measure the cell viability of HT-29 cells under various treatments with conditioned medium (CM) and oxaliplatin. (e) The alamarBlue assay was used to measure the cell viability of the HT-29 *RAB31* overexpression cell model combined with GW4869 in response to oxaliplatin treatment. (f) An evaluation of the synergistic effect of GW4869 and oxaliplatin on HT-29 *RAB31* expression levels was plotted. ** $p < 0.01$, *** $p < 0.001$ compared to vehicle group by Student's *t*-test.

observed as drug-resistant cells, whereas HT-29 cells were deemed sensitive. Combined with previous qPCR results (Figure 2b), cells expressing low levels of *RAB31*, such as HT-29, exhibited lower IC₅₀ values, while those expressing high levels of *RAB31*, such as SW1116, displayed increased resistance to oxaliplatin treatment. Our experimental findings demonstrate a trend similar to that of the GDSC profiles (Figure 3b). In our *RAB31* knockdown cell model, we significantly reduced the IC₅₀ of oxaliplatin (Figure 3c).

To confirm the association of these events with the exocytotic properties of *RAB31*, we analysed the conditioned medium from the *RAB31* overexpression model, which demonstrated heightened resistance to oxaliplatin in colorectal cancer (see Figure 3d). Conversely, introducing the exocytosis inhibitor GW4869 into the *RAB31* overexpression model considerably enhanced the response to oxaliplatin (Figure 3e). More importantly, oxaliplatin and GW4869 exhibited synergistic effects in a colorectal cancer model with *RAB31* overexpression (Figure 3f and Figure S4). Taken together, these findings suggest that *RAB31* expression enhances exocytosis, giving rise to drug resistance.

3.4 | EMT and *RAB31* form a regulatory loop that promotes exocytosis and metastasis

During the process of epithelial-to-mesenchymal transition (EMT), changes in tissue morphology occur, while mesenchymal-type cells facilitate drug resistance and exocytosis, which can ultimately lead to tumour metastasis. These factors are widely acknowledged in literature (Islam et al., 2022; Park et al., 2022). In this study, we aimed to examine the association between *RAB31* expression and both mesenchymal and epithelial markers in CRC patients with colorectal cancer. The study found a positive correlation between the *RAB31* gene's expression in colorectal cancer and the mesenchymal markers *CDH2* ($R = 0.84$), *SNAI2* ($R = 0.9$), *TWIST1* ($R = 0.85$), and *SNAI1* ($R = 0.61$) (Figure S5A). In addition, gene expression was negatively correlated with EMT-related microRNA miR-203a-3p ($R = -0.350$) in the clinical population (Quiñones-Díaz et al., 2020) (Figure S5B) and displayed an inverse correlation with the epithelial-type markers *CDH1* ($R = -0.095$) and *TJP3* ($R = -0.31$) (Figure S5C). Not only do we detect expression of EMT molecules, but we also calculate the previously defined “EMT Score” algorithm by scientists (Salt et al., 2014). We studied the transcriptome profiles of 34 CRC cell lines (GSE36133), extracted EMT markers and *RAB31* expression and observed a positive correlation between EMT score and *RAB31* expression (Figure S6 and Table S1).

To verify whether the association between *RAB31* and the EMT score in the clinical data above could be demonstrated in the colorectal cancer cell expression profile, we assessed the expression levels of *RAB31* and EMT-enabling genes, which had been evaluated for their corresponding EMT score (Matsuda et al., 2016), in the colorectal cancer cells (Figure 4a). Additionally, we evaluated the increased migratory and invasive potential of colorectal cancer cells following the overexpression of *RAB31* (Figure 4b). Additionally, the luciferase reporter gene assay demonstrated the restoration of E-cadherin promoter activity in the *RAB31* knockdown model, and vice versa (Figure 4c). Upon *RAB31* overexpression, the integration of multiple target genes (*CDH1*, *TJPI*, *SNAI2*, *SNAI1*, *VIM*, *TWIST1* and *miR-18a*) was verified through qPCR, with a trend of EMT observed (Figure 4d). Slug and vimentin expression was upregulated by *RAB31* overexpression (Figure 4e), whereas they were downregulated by *RAB31* knockdown (Figure 4f). Adding the exocytosis inhibitor GW4869 to the overexpression model also suppressed EMT (Figure 4g and Figure S7). Based on these findings, we can conclude that there is a relationship between *RAB31* expression, exocytosis, and EMT.

3.5 | *RAB31* is involved in ESCRT-independent pathways and facilitates the fusion and release of AGR2

To explain the role of *RAB31* in EV secretion and EMT, we posited that *RAB31* and its interaction partners regulate membrane fusion and exocytosis. We first used EM (electron microscope) imaging to observe cell morphology and vesicle formation. In the *RAB31* overexpression model, we found that there were more vesicles such as MVBs, ILVs and lysosomes (Figure 5a) and NTA proved that the *RAB31* overexpression group could produce more vesicles (Figure S8). We also observed a significant increase in the fluorescent signal of EV-specific membrane protein markers isolated from the *RAB31* overexpression model compared to the vector group (Figure 5b). Previous findings suggest that *RAB31* cuts through an ESCRT-independent exocytosis pathway (Narumi et al., 2015; Tomoshige et al., 2018; Wodziak et al., 2016). Therefore, we analysed several ESCRT-dependent and independent molecules to identify this signature. The *RAB31* overexpression models exhibited significantly elevated ESCRT-independent markers such as *FLOT1/2*, *CD63* and *TBC1D2B* compared to controls (Figure 5c). We opted for *VPS24* and *FLOT1* shRNA to interfere with the exocytosis process. *FLOT1* knockdown can bring about more significant changes in particle intensity/size (Figure 5d), EV-related miRNA expression (Figure 5e), EMT marker expression (Figure 5f) and cell migration ability (Figure 5g). The evidence supports the findings that *RAB31* depends on the ESCRT-independent model to promote cancer cell exocytosis.

We investigated whether EVs associate with fusion components or interaction partners other than *RAB31*-EGFR. We analysed the *RAB31* interactome, concentrating on eight membrane candidates: *ABCC2*, *EGFR*, *TCTN2/TCTN3*, *CD55*, *FLOT1*, *AGR2*, *STX7* and *NCSTN* (Figure 6a). Among these candidates, we observed a notable increase in *AGR2* expression in both intracellular and isolated EVs. Further analysis revealed a direct interaction between *AGR2* and *RAB31* using a two-way immunoprecipitation assay (Figure 6c). Additionally, an increase in *AGR2* was observed in the model utilising EGF to catalyse EGFR-regulated exocytosis (Figure 6d). Notably, the phosphorylation status of EGFR and EGF stimulation had no significant impact on *AGR2* function (Hong et al., 2021). To demonstrate the impact of *AGR2* inhibition, we observed that *RAB31*-induced EMT was inhibited upon the downregulation of *AGR2* (Figure 6e). Additionally, we detected heightened arginase activity, indicative of highly

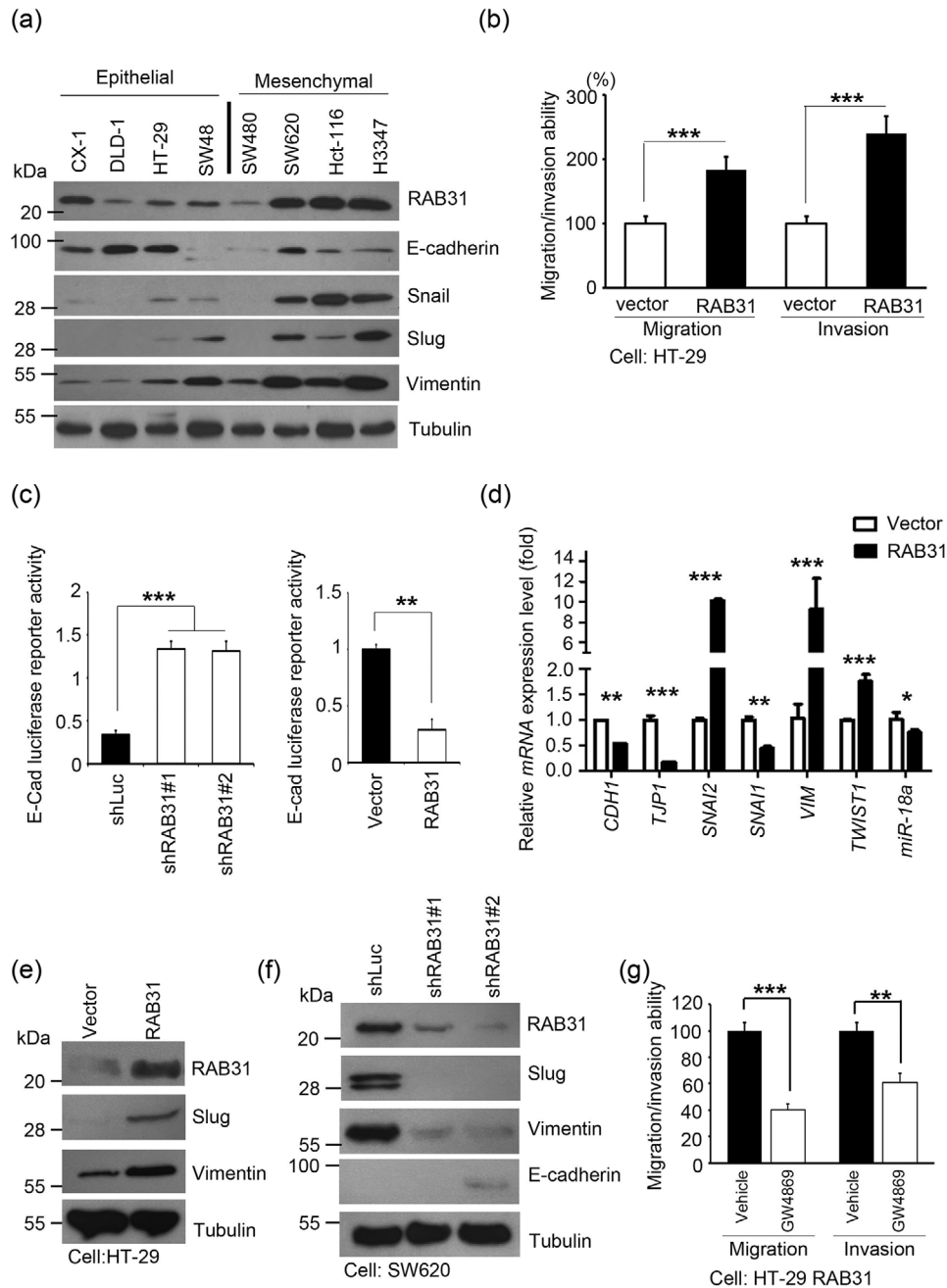


FIGURE 4 Interaction between *RAB31* and EMT-related molecules in colorectal cancer cell lines. (a) Western blots expressing *RAB31*, E-cadherin, Snail, Slug and Vimentin in a panel of colorectal cancer cells. (b) Migration/invasion ability (%) in HT-29 cells with or without *RAB31* overexpression plasmids. (c) Luciferase reporter activity of the E-cadherin molecule in models of *RAB31* overexpression and *RAB31* knockdown colorectal cancer, respectively. (d) qPCR analysis was performed for the expression of EMT-related markers (*CDH1*, *TJP1*, *SNAI2*, *SNAI1*, *VIM*, *TWIST1* and miR-18a) in the *RAB31* expression model. (e) Western blots showing the *RAB31*, Slug, and Vimentin in HT-29 cells with or without *RAB31* overexpression plasmids. (f) Western blots showing the *RAB31*, Slug, Vimentin and E-cadherin in SW620 cells with or without sh*RAB31* clones. (g) Migration/invasion ability in models of overexpression of HT-29 *RAB31* with or without GW4869 treatment. EMT, epithelial-mesenchymal transition; qPCR, quantitative polymerase chain reaction, * $p < 0.05$, ** $p < 0.01$, *** $p < 0.001$ compared to vehicle group by Student's *t*-test.

activated AGR2 function, with a significant increase upon *RAB31* overexpression. This activity was fully compromised by the use of the dominant-negative S19N mutant form (Yeo et al., 2015) (Figure 6f). Using the same cell model, the multiplex model conspicuously observed fusion at the membrane area, while the control or dominant negative models did not exhibit identical results (Figure 6g). Our model manipulations show that overexpression of *RAB31* increases exocytosis in cancer cells and that *RAB31* also leaves the cell upon fusion with the EV membrane.

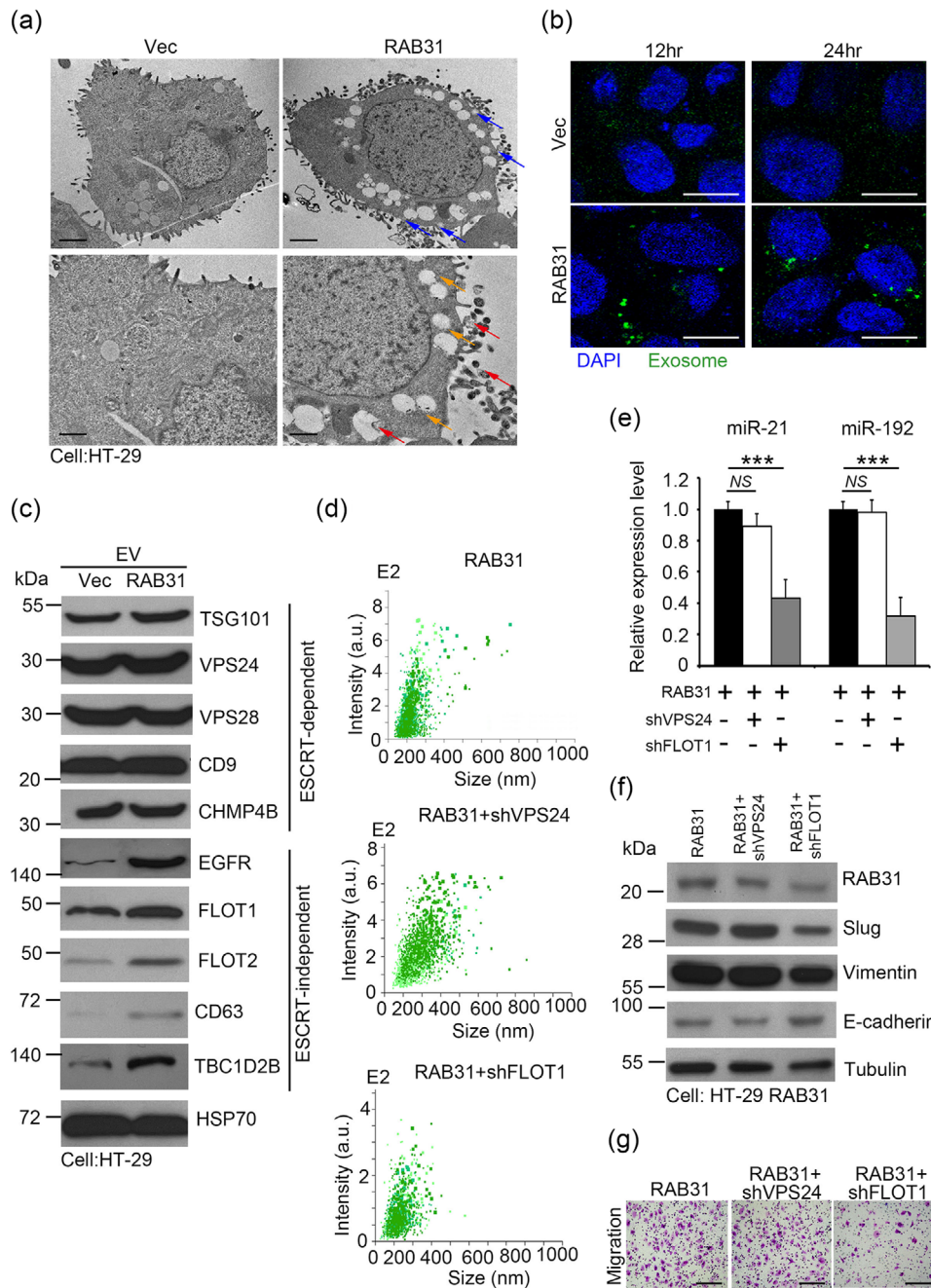


FIGURE 5 *RAB31* plays a role in the exocytosis pathway, which operates independently from ESCRT. (a) Representative images of *RAB31*-expression model in HT-29 cells examined by transmission electron microscopy (TEM). Blue arrows indicate exocytosis; yellow and red arrows indicate ILVs and MVBs, respectively. Scale bar: 1 μm and 0.5 μm , respectively. (b) Representative images of exosomes between vector and *RAB31*-overexpression models in HT-29 cells examined by confocal microscopy. Analysis represents exosomal membranes. Blue: DAPI. Green: exosome membrane. Scale bar: 25 μm . (c) Western blots showing the ESCRT-dependent molecules (TSG101, VPS24, VPS28, CD9 and CHMP4B) and ESCRT-independent molecules (EGFR, FLOT1/2, CD63 and TBC1D2B) in EVs isolated from *RAB31* overexpression models. HSP70 was used as an internal control. (d) EV concentration (particles/ml) and intensity (a.u.) of the HT-29 *RAB31* overexpressing cells with or without VPS24 and FLOT shRNA treatment were examined by nanoparticle tracking analysis (NTA). (e) qPCR analysis of *miR-21* and *miR-192* expression in EVs isolated from *RAB31* overexpression models with or without VPS24 and FLOT shRNA treatment. (f) Western blots showing *RAB31*, Slug, Vimentin and E-cadherin in HT-29 *RAB31* overexpressing cells with or without VPS24 and FLOT shRNA treatment. Tubulin was used as an internal control. (g) Migration ability of HT-29 *RAB31* overexpressing cells with or without VPS24 and FLOT shRNA treatment. ESCRT, endosomal sorting complex required for the transport; EV, extracellular vesicle; ILVs, intraluminal vesicles; MVBs, multivesicular bodies. ** $p < 0.01$, *** $p < 0.001$ compared to the vehicle group by Student's *t*-test.

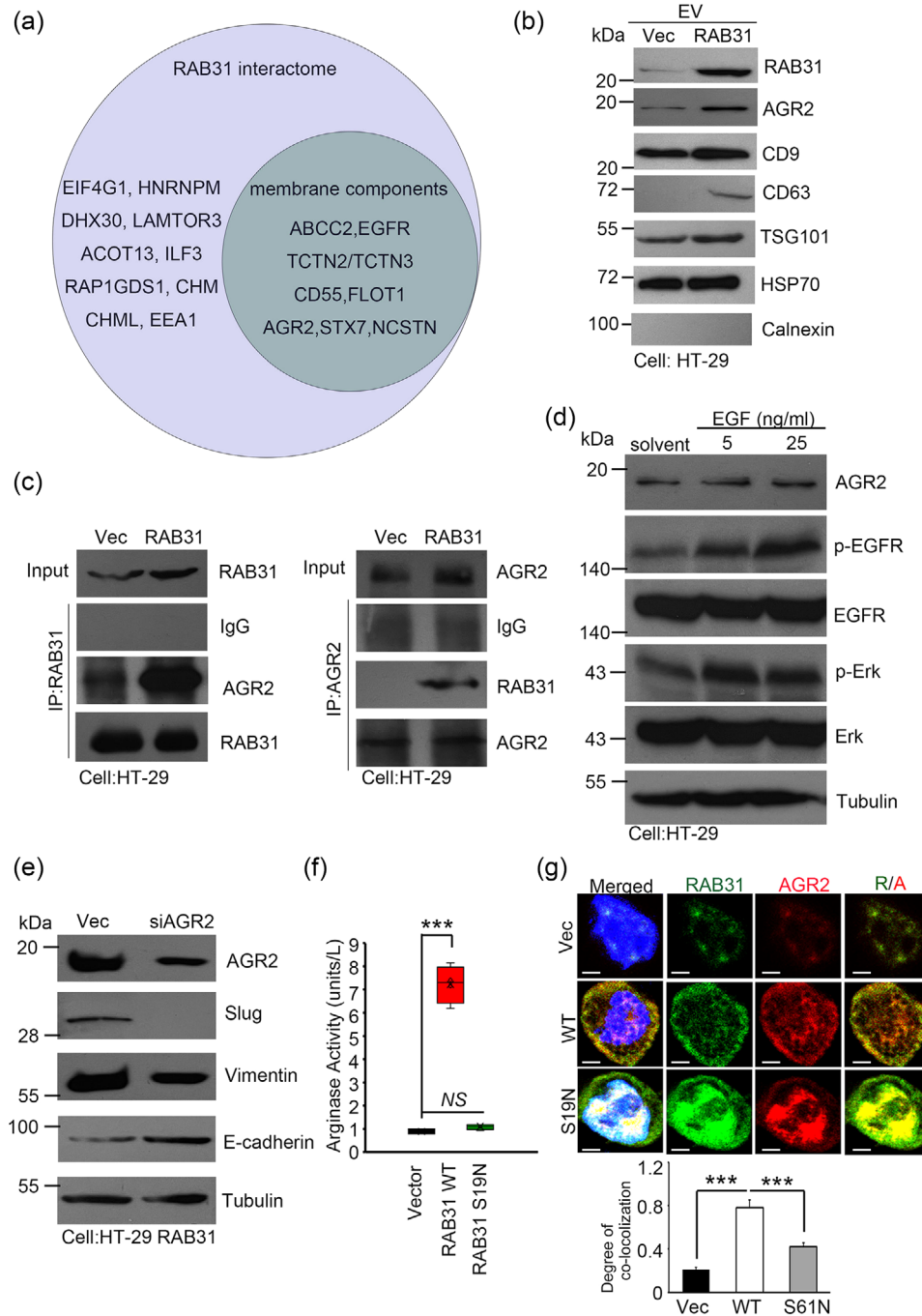


FIGURE 6 RAB31 fuses AGR2 into vesicles that target Epidermal Growth Factor Receptor (EGFR)-directed ESCRT-independent vesicles. (a) Venn diagram indicates RAB31 interaction partners and only molecules in the membrane location. (b) Western blots detect RAB31/AGR2 expression and EV-related molecules (CD9, CD63, TSG101) in EV isolated from HT-29 cells with or without RAB31 overexpression. (c) Immunoprecipitation analysis of the protein interaction affinity between RAB31 and AGR2 in HT-29 RAB31 overexpression models. (d) Western blots detected AGR2, phosphor/total-EGFR and phosphor/total-Erk expression in HT-29 cells with or without EGF (5–25 ng/ml) treatment. Actin was used as an internal control. (e) Western blots detected AGR2, Slug, Vimentin and E-cadherin expression in HT-29 RAB31 cells with or without siAGR2 transfected. Actin was used as an internal control. (f) Arginase activity was detected between vector, RAB31 wild-type and RAB31 S19N expression models. (g) Immunofluorescence signals of RAB31, AGR2 and DAPI among vector, RAB31 wild-type and RAB31 S19N expression models were detected by confocal microscopy. The degree of colocalisation of RAB31/AGR2 in membrane regions was quantified by Metamorph software. ESCRT, endosomal sorting complex required for the transport; EV, extracellular vesicle. *** $p < 0.001$ compared to vehicle group by Student's t -test.

3.6 | *RAB31* is found to impact cancer-associated fibroblast (CAF) development and presentation by means of AGR2 discharge

In addition to facilitating malignant progression and metastasis in tumours, exocytosis releases factors that induce reprogramming of the tumour microenvironment and alter immune infiltration. To investigate this, we used a bioinformatics algorithm to examine the expression of *RAB31* and various immune responses. Our findings revealed a positive correlation between *RAB31* and CAFs in colon cancer (Figure 7a). Additionally, scatter plots were analysed using four distinct statistical models that revealed reliable patterns between *RAB31* expression levels and infiltration levels (Figure 7b). Notably, CAF events were a significant independent prognostic factor in colorectal cancer (Figure 7c).

We developed a culture system comprising colorectal cancer cell lines and fibroblasts using several established canonical CAF biomarkers. After adding condition medium in the *RAB31* overexpression group, CAF markers were upregulated compared with the control group (Figure 7d). Furthermore, the conditioned medium (CM) of the treated cells (CAF-CM) significantly enhanced the migration capacity of the colorectal cancer cell lines (Figure 7e). Likewise, we recruited dominant negative *RAB31* (S19N) and shAGR2. CAF labelling previously elevated by addition of conditioned medium in which *RAB31* was overexpressed was reversed (Figure 7f). Based on this evidence, we demonstrated that the fusion of *RAB31* with EGFR/AGR2 during exocytosis and EMT is a hastened process that induces oxaliplatin resistance and CAF development (Figure 7g). This finding warrants further attention in the treatment and research of colorectal cancer.

4 | DISCUSSION

Irinotecan and oxaliplatin are currently the most prevalent drugs used to treat advanced colorectal cancer because of their ability to damage DNA replication, hindering the growth of cancerous cells. Objective statistics indicate that approximately 30%–40% of patients experience relapse and drug resistance, calling for a need to seek an efficient target to enhance drug resistance and thus benefit colon cancer patients (Duineveld et al., 2016). This is primarily due to drug resistance, as prescribed therapeutic drugs cannot inhibit the progression of cancer cells. In this study, we propose a primary role for *RAB31* in the profiling of oxaliplatin and irinotecan in drug-resistant cell lines. Clinical analysis of TCGA indicated a significantly different recurrence-free survival outcome ($p = 0.047$) when *RAB31* was increased in colorectal cancer. *RAB31* expression was consistently induced in colorectal cancer cells exposed to an oxaliplatin environment, as observed in various genetic profiles. During this period, *RAB31* continued to show an upward trend until the cells developed drug resistance. Studies have shown that upregulation of *RAB31* is associated with oxaliplatin resistance in colorectal cancer (Zheng et al., 2015).

RAB31 has been implicated in numerous malignancies in previous studies (Li et al., 2019). It is the most researched marker for breast cancer (Chua & Tang, 2015). The expression of *RAB31* is linked to poor prognosis, particularly among those with the ER⁺ subtype (Jin et al., 2012; Kotsch et al., 2008; 2017). Additionally, it has been demonstrated that MCU1 regulates *RAB31*, and when overexpressed, *RAB31* promotes increased proliferation and sphere formation in breast cancer cells (Young et al., 2010). The effects of *RAB31* on cell growth and death have been reported in gastric cancer and glioblastoma (Chen et al., 2018; Pan et al., 2016). *RAB31* regulates miR-30c-2-3p, which controls GLI1 and subsequently influences the growth and death of gastric cancer cells. *RAB31* may also be regulated by RAI14 (Chen et al., 2018). A recent study showed that overexpression of *RAB31* leads to reduced efficacy of bortezomib and increased anti-apoptotic activity (Yoon et al., 2019), suggesting that *RAB31* promotes drug resistance in various cancers. Researchers have discovered that Rab proteins are associated with multidrug resistance in various types of cancers. This indicates that the overexpression of Rab proteins can affect cancer cell resistance to drugs (Engstrand et al., 2018; Gopal Krishnan et al., 2020; Han et al., 2020). Notably, this study is the first to describe the potential role of *RAB31* in oxaliplatin resistance. EMT is a cellular mechanism that responds to environmental changes such as drug stimulation. The role of *RAB31* in regulating tumour growth through the mTOR/p70S6K/Cyclin D1 pathway has been demonstrated in colorectal cancer (Yang et al., 2020). However, the link between colorectal cancer and EMT has not yet been investigated. Both microarray and clinical studies have demonstrated that *RAB31* is significantly associated with mesenchymal markers and inversely associated with epithelial markers in colorectal cancer. We need to continue to explore whether *RAB31* affects EMT and E-cadherin directly or through indirect regulatory mechanisms. Our next step will be to extract the miRNAs or mRNAs involved in EVs to demonstrate that they play important roles in E-cadherin expression and EMT. In addition to the targets detected in this study, we will also establish RNA-seq and ChIP-seq for demonstration in further experiments. *RAB31* expression has been confirmed in many colorectal cancer cell lines, which is consistent with clinical data that may indicate variations in morphology during the EMT process. The expression of *RAB31* has been demonstrated to affect cell growth and motility in various cancer types such as esophageal squamous cell carcinoma, osteosarcoma and cervical cancer (Huang et al., 2022; Liu et al., 2018; Wu et al., 2020). Establishing a *RAB31*-based model confirmed a correlation between the expression of E-cadherin and mesenchymal-related molecules (SNAI2, VIM and TWIST1) at the RNA and protein levels in colorectal cancer cells and *RAB31* biological function. Evidence suggests that EMT mediated by *RAB31* contributes to oxaliplatin resistance in colorectal cancer. Furthermore, the level of *RAB31* in cells was found

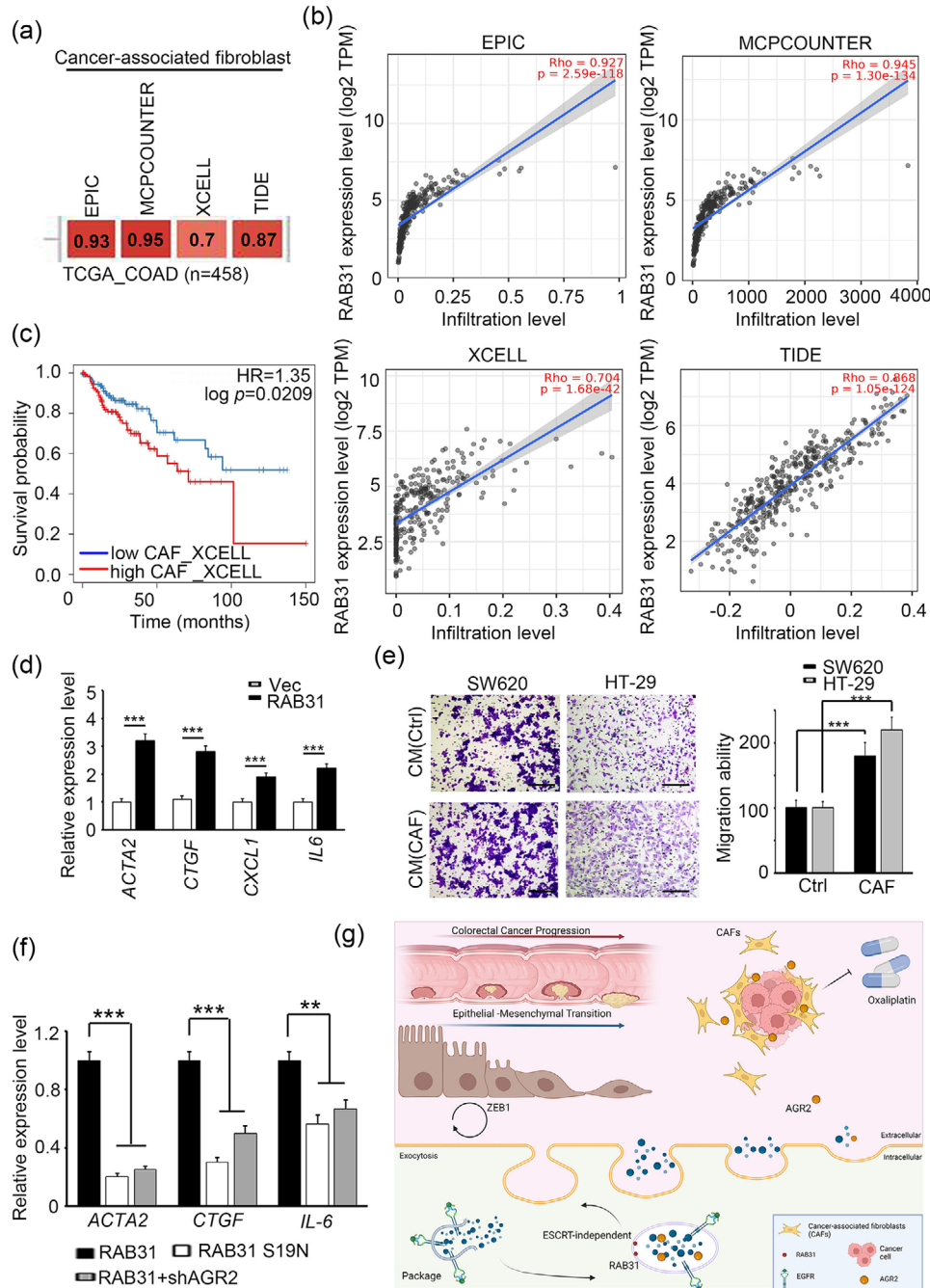


FIGURE 7 *RAB31* regulates CAF formation and metastatic capacity through secretion of AGR2. (a) The correlation between *RAB31* expression levels and cancer-associated fibroblast events was investigated by several statistical algorithms. The predictions and calculations are from the TIMER website. (b) The scatter plot between *RAB31* expression levels and cancer-associated fibroblast events was investigated by several statistical algorithms (EPIC, MCPCOUNTER, XCELL and TIDE). The predictions and calculations are from the TIMER website. (c) Kaplan-Meier analysis of the percentage of CAF with concomitant low or high levels determined algorithmically by the TIMER website at the endpoint of overall survival probability in patients with colon adenocarcinoma. (d) qPCR analysis of *ACTA2*, *CTGF*, *CXCL1* and *IL-6* expression in CAF cells after adding HT-29 vector or *RAB31* overexpression conditioned medium. (e) Migration ability of SW620 and HT-29 cells combined with control or CAF-conditioned medium, respectively. (f) qPCR analysis of *ACTA2*, *CTGF* and *IL-6* expression in CAF cells after adding HT-29 *RAB31* with wild-type, mutant, and wild-type combined shAGR2, respectively. (g) Schematic representation of fusion vesicles and mechanisms of resistance to oxaliplatin resistance in the dynamic progression of colon cancer. CAF, cancer-associated fibroblasts; qPCR, quantitative polymerase chain reaction. *** $p < 0.001$ compared to vehicle group by Student's *t*-test.

to be correlated with the IC50 of oxaliplatin, as established by the relationship between cells and IC50. Knocking down *RAB31* increased cell sensitivity to oxaliplatin. The findings of this study support the hypothesis that *RAB31* modifies the morphology and drug responses of colorectal cancer cells.

Recently, the tumour microenvironment has been suggested as a means to promote tumour cells to evade suppression by both drug therapy and the immune system (Wei et al., 2021; Zheng et al., 2020). In this context, EVs secretion plays a critical role and may serve as a promising therapeutic target for colorectal cancer. (Li et al., 2019; Pan et al., 2016). Studies have shown that EVs serve as a means of communication between tumour cells and surrounding cells (Zhang et al., 2022). Rab proteins have been implicated in membrane-related physiological functions such as exocytosis (Banworth & Li, 2018; Hendrix et al., 2010). In our study, we showed that *RAB31* overexpression led to an increase in RNA and protein levels, suggesting an increase in exocytosis efficacy. Upon inhibiting extracellular vesicle (EV) function, we observed a reversal of *RAB31*-mediated epithelial-mesenchymal transition processes and a consequent change in cellular resistance to oxaliplatin drugs. Moreover, it is noteworthy that evidence supporting the use of EV inhibitors indicates that they synergistically enhance cell sensitivity to oxaliplatin drugs. This finding supports the idea that *RAB31* plays a crucial role in altering EMT phenotypes and drug resistance. Whether EMT or oxaliplatin, there is growing evidence that EVs and their cargo, including long non-coding RNAs, miRNAs and some DNA fragments, may be released and involved. In this study, we roughly detected several targets already mentioned, such as EMT-related target, miR21 and miR-192 (Figure S3), as well as oxaliplatin resistance-related molecules, such as CPT1A and miR-1915-3p (Figure S9) (Lin et al., 2021; Xiao et al., 2021). We are using NGS technology to further reveal differentially expressed genes (DEGs) through EV isolation and try to find more candidate genes.

Rab protein-mediated membrane transport is required for interactions with diverse proteins (D'Adamo et al., 2014). Through interactome analysis, several new partners of *RAB31* have been identified in colorectal cancer. In previous studies, AGR2's distribution exhibited was positively correlated with EGFR, potentially enabling stimulation of EGFR signalling. Additionally, *RAB31* may have the ability to guide EGFR towards multivesicular endosomes (Narumi et al., 2015; Tomoshige et al., 2018; Wodziak et al., 2016). However, we discovered that AGR2 directly interacts with *RAB31* and contributes to EMT and exocytosis in colorectal cancer, which are unrelated to EGFR signalling. Furthermore, AGR2 has been linked to unfavorable prognosis in colorectal cancer, and activation of the Wnt/ β -catenin axis can prompt AGR2 to promote stem cell activity (Dahal Lamichane et al., 2019). The study results suggest that AGR2 affects not only the *RAB31* interaction, but also EMT and exocytosis in colorectal cancer. Despite overexpression of *RAB31* activating EGFR signalling, AGR2 protein levels remained unaffected by inhibition of EGFR signalling, and Rab-31-mediated resistance to oxaliplatin persisted.

Previous studies have shown that cancer-associated fibroblasts mediate the extracellular form of *RAB31*, thereby driving the progression of colorectal cancer. More research is required to determine the function of *RAB31* in the tumour microenvironment (Yang et al., 2020). To fill this knowledge gap, our study proposes that EVs could be one mechanism by which *RAB31* influences drug resistance in colorectal cancer. In summary, our findings contribute to the understanding of *RAB31* in the tumour microenvironment. The use of *RAB31* represents a promising target for investigating drug resistance in colorectal cancer and may offer an alternative therapy.

AUTHOR CONTRIBUTIONS

Conception and design: Yu-Chan Chang, Ming-Huang Chen, Chi-Long Chen and Michael Hsiao. *Development of methodology:* Yu-Chan Chang, Chien-Hsiu Li, Ming-Hsien Chan and Yi-Fang Yang. *Acquisition of data (provided animals, acquired and managed patients, and provided facilities):* Yu-Chan Chang, Chien-Hsiu Li, Ming-Hsien Chan, Yi-Fang Yang and Meng-Lun Lu. *Data analysis and interpretation (e.g., statistical analysis, biostatistics, computational analysis):* Yu-Chan Chang, Chien-Hsiu Li, Ming-Hsien Chan and Yi-Fang Yang. *Writing, review, and/or revision of the manuscript:* Yu-Chan Chang, Chien-Hsiu Li, Ming-Hsien Chan, Yi-Fang Yang, Ming-Huang Chen, Chi-Long Chen and Michael Hsiao. *Administrative, technical, or material support (i.e., reporting or organizing data, constructing databases):* Ming-Huang Chen and Chi-Long Chen. *Study supervision:* Michael Hsiao.

ACKNOWLEDGEMENTS

We would like to thank the GRC Instrument Core Facilities for their support with the Affymetrix microarray, IVIS spectrum, Aperio digital pathology analyses, and AS-EM core facility. This study was supported by the Ministry of Science and Technology [MOST 111-2320-B-038-061] and [NSTC 112-2320-B-038-048] to C. L. Chen.

CONFLICT OF INTEREST STATEMENT

The authors disclosed no conflicts.

CRC tissues were recovered from the Department of Pathology, Taipei Municipal Wan Fang Hospital (Taipei, Taiwan), with approval from the Institutional Review Board (TMU-IRB 99049).

DATA AVAILABILITY STATEMENT

The datasets used and/or analysed during the current study are available from the corresponding author upon reasonable request.

ORCID

Michael Hsiao  <https://orcid.org/0000-0001-8529-9213>

REFERENCES

- Abrams, T. A., Meyer, G., Schrag, D., Meyerhardt, J. A., Moloney, J., & Fuchs, C. S. (2014). Chemotherapy usage patterns in a US-wide cohort of patients with metastatic colorectal cancer. *Journal of the National Cancer Institute*, *106*(2), djt371.
- Banworth, M. J., & Li, G. (2018). Consequences of Rab GTPase dysfunction in genetic or acquired human diseases. *Small GTPases*, *9*(1-2), 158–181.
- Bartha, Á., & Györfy, B. (2021). TNMplot.com: A web tool for the comparison of gene expression in normal, tumor and metastatic tissues. *International Journal of Molecular Sciences*, *22*(5), 2622.
- Chang, Y. C., Chiou, J., Yang, Y. F., Su, C. Y., Lin, Y. F., Yang, C. N., Lu, P. J., Huang, M. S., Yang, C. J., & Hsiao, M. (2019). Therapeutic targeting of aldolase a interactions inhibits lung cancer metastasis and prolongs survival. *Cancer Research*, *79*(18), 4754–4766.
- Chang, Y. C., Li, C. H., Chan, M. H., Fang, C. Y., Zhang, Z. X., Chen, C. L., & Hsiao, M. (2023). Overexpression of synaptic vesicle protein Rab GTPase 3C promotes vesicular exocytosis and drug resistance in colorectal cancer cells. *Molecular Oncology*, *17*(3), 422–444.
- Chang, Y. C., Su, C. Y., Chen, M. H., Chen, W. S., Chen, C. L., & Hsiao, M. (2017). Secretory RAB GTPase 3C modulates IL6-STAT3 pathway to promote colon cancer metastasis and is associated with poor prognosis. *Molecular Cancer*, *16*(1), 135.
- Chang, Y. T., Peng, H. Y., Hu, C. M., Huang, S. C., Tien, S. C., & Jeng, Y. M. (2020). Pancreatic cancer-derived small extracellular vesical Ezrin regulates macrophage polarization and promotes metastasis. *American Journal of Cancer Research*, *10*(1), 12–37.
- Chen, C., Maimaiti, A., Zhang, X., Qu, H., Sun, Q., He, Q., & Yu, W. (2018). Knockdown of RAI14 suppresses the progression of gastric cancer. *OncoTargets and Therapy*, *11*, 6693–6703.
- Chiba, M., Kimura, M., & Asari, S. (2012). Exosomes secreted from human colorectal cancer cell lines contain mRNAs, microRNAs and natural antisense RNAs, that can transfer into the human hepatoma HepG2 and lung cancer A549 cell lines. *Oncology Reports*, *28*(5), 1551–1558.
- Chua, C. E., & Tang, B. L. (2015). The role of the small GTPase Rab31 in cancer. *Journal of Cellular and Molecular Medicine*, *19*(1), 1–10.
- D'Adamo, P., Masetti, M., Bianchi, V., Morè, L., Mignogna, M. L., Giannandrea, M., & Gatti, S. (2014). RAB GTPases and RAB-interacting proteins and their role in the control of cognitive functions. *Neuroscience and Biobehavioral Reviews*, *46*(Pt (2)), 302–314.
- Dahal Lamichane, B., Jung, S. Y., Yun, J., Kang, S., Kim, D. Y., Lamichane, S., Kim, Y. J., Park, J. H., Jang, W. B., Ji, S. T., Dehua, L., Ha, J. S., Kim, Y. H., & Kwon, S. M. (2019). AGR2 is a target of canonical Wnt/ β -catenin signaling and is important for stemness maintenance in colorectal cancer stem cells. *Biochemical and Biophysical Research Communications*, *515*(4), 600–606.
- Duineveld, L. A., van Asselt, K. M., Bemelman, W. A., Smits, A. B., Tanis, P. J., van Weert, H. C., & Wind, J. (2016). Symptomatic and asymptomatic colon cancer recurrence: A multicenter cohort study. *Annals of Family Medicine*, *14*(3), 215–220.
- Engstrand, J., Nilsson, H., Strömberg, C., Jonas, E., & Freedman, J. (2018). Colorectal cancer liver metastases—A population-based study on incidence, management and survival. *BMC cancer*, *18*(1), 78.
- Erami, Z., Khalil, B. D., Salloum, G., Yao, Y., LoPiccolo, J., Shymanets, A., Nürnberg, B., Bresnick, A. R., & Backer, J. M. (2017). Rac1-stimulated macropinocytosis enhances G $\beta\gamma$ activation of PI3K β . *The Biochemical Journal*, *474*(23), 3903–3914.
- Gopal Krishnan, P. D., Golden, E., Woodward, E. A., Pavlos, N. J., & Blancafort, P. (2020). Rab GTPases: Emerging oncogenes and tumor suppressive regulators for the editing of survival pathways in cancer. *Cancers*, *12*(2), 259.
- Han, J., Sun, W., Liu, R., Zhou, Z., Zhang, H., Chen, X., & Ba, Y. (2020). Plasma exosomal miRNA expression profile as oxaliplatin-based chemoresistant biomarkers in colorectal adenocarcinoma. *Frontiers in Oncology*, *10*, 1495.
- Hendrix, A., & Hume, A. N. (2011). Exosome signaling in mammary gland development and cancer. *The International Journal of Developmental Biology*, *55*(7-9), 879–887.
- Hendrix, A., Westbroek, W., Bracke, M., & De Wever, O. (2010). An ex(o)citing machinery for invasive tumor growth. *Cancer Research*, *70*(23), 9533–9537.
- Homma, Y., Hiragi, S., & Fukuda, M. (2021). Rab family of small GTPases: An updated view on their regulation and functions. *The FEBS Journal*, *288*(1), 36–55.
- Hong, X., Li, Z. X., Hou, J., Zhang, H. Y., Zhang, C. Y., Zhang, J., Sun, H., Pang, L. H., Wang, T., & Deng, Z. H. (2021). Effects of ER-resident and secreted AGR2 on cell proliferation, migration, invasion, and survival in PANC-1 pancreatic cancer cells. *BMC Cancer*, *21*(1), 33.
- Huang, Y., Liu, R., Han, X., Hou, X., Tian, Y., & Zhang, W. (2022). Rab31 promotes the invasion and metastasis of cervical cancer cells by inhibiting MAPK6 degradation. *International Journal of Biological Sciences*, *18*(1), 112–123.
- Hutter, P. (2007). Rapidly evolving Rab GTPase paralogs and reproductive isolation in *Drosophila*. *Advances in Genetics*, *58*, 1–23.
- Islam, S. U., Ahmed, M. B., Sonn, J. K., Jin, E. J., & Lee, Y. S. (2022). PRP4 induces epithelial-mesenchymal transition and drug resistance in colon cancer cells via activation of p53. *International Journal of Molecular Sciences*, *23*(6), 3092.
- Jalagadugula, G., Mao, G., Goldfinger, L. E., Wurtzel, J., Del Carpio-Cano, F., Lambert, M. P., Estevez, B., French, D. L., Poncz, M., & Rao, A. K. (2022). Defective RAB31-mediated megakaryocytic early endosomal trafficking of VWF, EGFR, and M6PR in RUNX1 deficiency. *Blood Advances*, *6*(17), 5100–5112.
- Jin, C., Rajabi, H., Pitroda, S., Li, A., Kharbanda, A., Weichselbaum, R., & Kufe, D. (2012). Cooperative interaction between the MUC1-C oncoprotein and the Rab31 GTPase in estrogen receptor-positive breast cancer cells. *PLoS ONE*, *7*(7), e39432.
- Jin, H., Tang, Y., Yang, L., Peng, X., Li, B., Fan, Q., Wei, S., Yang, S., Li, X., Wu, B., Huang, M., Tang, S., Liu, J., & Li, H. (2021). Rab GTPases: Central Coordinators of Membrane Trafficking in Cancer. *Frontiers in Cell and Developmental Biology*, *9*, 648384.
- Kotzsch, M., Kirchner, T., Soelch, S., Schäfer, S., Friedrich, K., Baretton, G., Magdolen, V., & Luther, T. (2017). Inverse association of rab31 and mucin-1 (CA15-3) antigen levels in estrogen receptor-positive (ER+) breast cancer tissues with clinicopathological parameters and patients' prognosis. *American Journal of Cancer Research*, *7*(9), 1959–1970.
- Kotzsch, M., Sieuwerts, A. M., Grosser, M., Meye, A., Fuessel, S., Meijer-van Gelder, M. E., Smid, M., Schmitt, M., Baretton, G., Luther, T., Magdolen, V., & Foekens, J. A. (2008). Urokinase receptor splice variant uPAR-del4/5-associated gene expression in breast cancer: Identification of rab31 as an independent prognostic factor. *Breast Cancer Research and Treatment*, *111*(2), 229–240.
- Li, H., Zhang, S. R., Xu, H. X., Wang, W. Q., Li, S., Li, T. J., Ni, Q. X., Yu, X. J., Liu, L., & Wu, C. T. (2019). SRPX2 and RAB31 are effective prognostic biomarkers in pancreatic cancer. *Journal of Cancer*, *10*(12), 2670–2678.
- Lin, D., Zhang, H., Liu, R., Deng, T., Ning, T., Bai, M., Yang, Y., Zhu, K., Wang, J., Duan, J., Ge, S., Sun, B., Ying, G., & Ba, Y. (2021). iRGD-modified exosomes effectively deliver CPT1A siRNA to colon cancer cells, reversing oxaliplatin resistance by regulating fatty acid oxidation. *Molecular Oncology*, *15*(12), 3430–3446.
- Liu, T., Zhang, X., Du, L., Wang, Y., Liu, X., Tian, H., Wang, L., Li, P., Zhao, Y., Duan, W., Xie, Y., Sun, Z., & Wang, C. (2019). Exosome-transmitted miR-128-3p increase chemosensitivity of oxaliplatin-resistant colorectal cancer. *Molecular Cancer*, *18*(1), 43.

- Liu, Y., Tang, Y., & Li, P. (2018). Inhibitory effect of microRNA-455-5p on biological functions of esophageal squamous cell carcinoma Eca109 cells via Rab31. *Experimental and Therapeutic Medicine*, 16(6), 4959–4966.
- Martínez-Morales, J. C., Romero-Ávila, M. T., Reyes-Cruz, G., & García-Sáinz, J. A. (2022). Roles of receptor phosphorylation and Rab proteins in G protein-coupled receptor function and trafficking. *Molecular Pharmacology*, 101(3), 144–153.
- Matsuda, Y., Miura, K., Yamane, J., Shima, H., Fujibuchi, W., Ishida, K., Fujishima, F., Ohnuma, S., Sasaki, H., Nagao, M., Tanaka, N., Satoh, K., Naitoh, T., & Unno, M. (2016). SERPIN11 regulates epithelial-mesenchymal transition in an orthotopic implantation model of colorectal cancer. *Cancer Science*, 107(5), 619–628.
- Narumi, S., Miki, Y., Hata, S., Ebina, M., Saito, M., Mori, K., Kobayashi, M., Suzuki, T., Iwabuchi, E., Sato, I., Maemondo, M., Endo, C., Inoue, A., Kondo, T., Yamada-Okabe, H., Ichinose, M., & Sasano, H. (2015). Anterior gradient 2 is correlated with EGFR mutation in lung adenocarcinoma tissues. *The International Journal of Biological Markers*, 30(2), e234–e242.
- Pan, Y., Zhang, Y., Chen, L., Liu, Y., Feng, Y., & Yan, J. (2016). The critical role of Rab31 in cell proliferation and apoptosis in cancer progression. *Molecular Neurobiology*, 53(7), 4431–4437.
- Park, Y. L., Kim, H. P., Ock, C. Y., Min, D. W., Kang, J. K., Lim, Y. J., Song, S. H., Han, S. W., & Kim, T. Y. (2022). EMT-mediated regulation of CXCL1/5 for resistance to anti-EGFR therapy in colorectal cancer. *Oncogene*, 41(14), 2026–2038.
- Quinones-Díaz, B. I., Reyes-González, J. M., Sánchez-Guzmán, V., Conde-Del Moral, I., Valiyeva, F., Santiago-Sánchez, G. S., & Vivas-Mejía, P. E. (2020). MicroRNA-18a-5p suppresses tumor growth via targeting matrix metalloproteinase-3 in cisplatin-resistant ovarian cancer. *Frontiers in Oncology*, 10, 602670.
- Salt, M. B., Bandyopadhyay, S., & McCormick, F. (2014). Epithelial-to-mesenchymal transition rewires the molecular path to PI3K-dependent proliferation. *Cancer Discovery*, 4(2), 186–199.
- Siegel, R. L., Miller, K. D., Fuchs, H. E., & Jemal, A. (2022). Cancer statistics, 2023. *CA: A Cancer Journal for Clinicians*, 72(1), 7–33.
- Spano, D., & Zollo, M. (2012). Tumor microenvironment: A main actor in the metastasis process. *Clinical & Experimental Metastasis*, 29(4), 381–395.
- Stenmark, H. (2009). Rab GTPases as coordinators of vesicle traffic. *Nature Reviews. Molecular Cell Biology*, 10(8), 513–525.
- Todosi, A. M., Gavriescu, M. M., Aniței, G. M., Filip, B., & Scripcariu, V. (2012). Colon cancer at the molecular level—Usefulness of epithelial-mesenchymal transition analysis. *Revista medico-chirurgicala a Societatii De Medici Si Naturalisti Din Iasi*, 116(4), 1106–1111.
- Tomoshige, K., Guo, M., Tsuchiya, T., Fukazawa, T., Fink-Baldauf, I. M., Stuart, W. D., Naomoto, Y., Nagayasu, T., & Maeda, Y. (2018). An EGFR ligand promotes EGFR-mutant but not KRAS-mutant lung cancer in vivo. *Oncogene*, 37(28), 3894–3908.
- Wei, D., Zhan, W., Gao, Y., Huang, L., Gong, R., Wang, W., Zhang, R., Wu, Y., Gao, S., & Kang, T. (2021). RAB31 marks and controls an ESCRT-independent exosome pathway. *Cell Research*, 31(2), 157–177.
- Wilson, T. R., Longley, D. B., & Johnston, P. G. (2006). Chemoresistance in solid tumours. *Annals of Oncology: Official Journal of the European Society for Medical Oncology*, 17(Suppl 10), x315–x324.
- Wodziak, D., Dong, A., Basin, M. F., & Lowe, A. W. (2016). Anterior gradient 2 (AGR2) induced epidermal growth factor receptor (EGFR) signaling is essential for murine pancreatitis-associated tissue regeneration. *PLoS ONE*, 11(10), e0164968.
- Wu, Q., Feng, Q., Xiong, Y., & Liu, X. (2020). RAB31 is targeted by miR-26b and serves a role in the promotion of osteosarcoma. *Oncology Letters*, 20(5), 244.
- Xiao, Z., Liu, Y., Li, Q., Liu, Q., Liu, Y., Luo, Y., & Wei, S. (2021). EVs delivery of miR-1915-3p improves the chemotherapeutic efficacy of oxaliplatin in colorectal cancer. *Cancer Chemotherapy and Pharmacology*, 88(6), 1021–1031.
- Yang, A. D., Fan, F., Camp, E. R., van Buren, G., Liu, W., Somcio, R., Gray, M. J., Cheng, H., Hoff, P. M., & Ellis, L. M. (2006). Chronic oxaliplatin resistance induces epithelial-to-mesenchymal transition in colorectal cancer cell lines. *Clinical Cancer Research: An Official Journal of the American Association for Cancer Research*, 12(14 Pt 1), 4147–4153.
- Yang, L., Tian, X., Chen, X., Lin, X., Tang, C., Gao, Y., Chen, S., & Ge, Z. (2020). Upregulation of Rab31 is associated with poor prognosis and promotes colorectal carcinoma proliferation via the mTOR/p70S6K/Cyclin D1 signalling pathway. *Life Sciences*, 257, 118126.
- Yang, T., Zhiheng, H., Zhanhuai, W., Qian, X., Yue, L., Xiaoxu, G., Jingsun, W., Shu, Z., & Kefeng, D. (2020). Increased RAB31 expression in cancer-associated fibroblasts promotes colon cancer progression through HGF-MET signaling. *Frontiers in Oncology*, 10, 1747.
- Ye, Z., Zhou, M., Tian, B., Wu, B., & Li, J. (2015). Expression of lncRNA-CCAT1, E-cadherin and N-cadherin in colorectal cancer and its clinical significance. *International Journal of Clinical and Experimental Medicine*, 8(3), 3707–3715.
- Yeo, J. C., Wall, A. A., Luo, L., & Stow, J. L. (2015). Rab31 and APPL2 enhance FcγR-mediated phagocytosis through PI3K/Akt signaling in macrophages. *Molecular Biology of the Cell*, 26(5), 952–965.
- Yoon, D., Bae, K., Kim, J. H., Choi, Y. K., & Yoon, K. A. (2019). Oncogenic effect of the novel fusion gene *VAPA-Rab31* in lung adenocarcinoma. *International Journal of Molecular Sciences*, 20(9), 2309.
- Young, J., Ménétrey, J., & Goud, B. (2010). RAB6C is a retrogene that encodes a centrosomal protein involved in cell cycle progression. *Journal of Molecular Biology*, 397(1), 69–88.
- Zhang, H., Xing, J., Dai, Z., Wang, D., & Tang, D. (2022). Exosomes: The key of sophisticated cell-cell communication and targeted metastasis in pancreatic cancer. *Cell Communication and Signaling: CCS*, 20(1), 9.
- Zheng, X., Ma, N., Wang, X., Hu, J., Ma, X., Wang, J., & Cao, B. (2020). Exosomes derived from 5-fluorouracil-resistant colon cancer cells are enriched in GDF15 and can promote angiogenesis. *Journal of Cancer*, 11(24), 7116–7126.
- Zheng, Y., Zhou, J., & Tong, Y. (2015). Gene signatures of drug resistance predict patient survival in colorectal cancer. *The Pharmacogenomics Journal*, 15(2), 135–143.

SUPPORTING INFORMATION

Additional supporting information can be found online in the Supporting Information section at the end of this article.

How to cite this article: Chang, Y.-C., Yang, Y.-F., Li, C.-H., Chan, M.-H., Lu, M.-L., Chen, M.-H., Chen, C.-L., & Hsiao, M. (2024). RAB31 drives extracellular vesicle fusion and cancer-associated fibroblast formation leading to oxaliplatin resistance in colorectal cancer. *Journal of Extracellular Biology*, 3, e141. <https://doi.org/10.1002/jex2.141>